Article

JOURNAL OF
biomaterials
applications

Journal of Biomaterials Applications
28(2) 241–249

DOI: 10.1177/0885328212445077
jba.sagepub.com
SAGE

Technique for internal channelling of hydroentangled nonwoven scaffolds to enhance cell penetration

Elaine R Durham[1], Eileen Ingham[2] and Stephen J Russell[1]

Abstract

An important requirement in thick, high-porosity scaffolds is to maximise cellular penetration into the interior and avoid necrosis during culture *in vitro*. Hitherto, reproducible control of the pore structure in nonwoven scaffolds has proved challenging. A new, channelled scaffold manufacturing process is reported based on water jet entanglement of fibres (hydroentangling) around filamentous template to form a coherent scaffold that is subsequently removed. Longitudinally-oriented channels were introduced within the scaffold in controlled proximity using 220 μm diameter cylindrical templates. In this case study, channelled scaffolds composed of poly(*l*-lactic acid) were manufactured and evaluated *in vitro*. Environmental scanning electron microscope and μCT (X-ray microtomography) confirmed channel openings in the scaffold cross-section before and after cell culture with human dermal fibroblasts up to 14 weeks. Histology at week 11 indicated that the channels promoted cell penetration and distribution within the scaffold interior. At week 14, cellular matrix deposition was evident in the internal channel walls and the entrances remained unoccluded by cellular matrix suggesting that diffusion conduits for mass transfer of nutrient to the scaffold interior could be maintained.

Keywords

Channels, scaffold, porosity, nonwoven, cell penetration

Introduction

Scaffolds for neo-tissue repair are required to support cell growth in three dimensions and should be highly porous with sufficient surface area for cell attachment and to allow continuous nutrient diffusion throughout.[1] The materials used to create the scaffold must be both biocompatible and degradable and until the neo-tissue becomes load bearing, the porosity should not compromise the mechanical performance.[2] A significant challenge in the repair of relatively thick, three-dimensional tissues is the extent to which depth-wise migration and colonisation of cells in the interior of a scaffold can be obtained. In soft tissue regeneration, formation of extracellular matrix (ECM) on the exterior of the scaffold can gradually reduce access of nutrient and oxygen to the interior of the scaffold, ultimately resulting in cell death and a necrotic core.[3,4] Practically, this limits the thickness of tissue that can be regenerated.[5]

One approach that has been explored to increase cell infiltration and nutrient access to the interior has been the introduction of channels within the scaffold structure.[6–8] Techniques have been developed for introducing channels in sponge, foam and hydrogel,[9–11] but not in nonwoven scaffolds. The introduction of channels also aims to overcome limitations in the pore structure of certain scaffold types. Porogen-fused scaffolds typically have limited pore interconnectivity, which affects nutrient diffusion.[12,13] Similarly, in hydrogels, the density required to form a mechanically stable construct can negatively influence nutrient diffusion.[14,15] The introduction of tubular channels has been reported in hydroxyapatite scaffolds for tissue engineering of bone[9] as well as to improve cell distribution in porous poly(l-lactic acid) (PLA) scaffolds produced using solid–liquid phase separation techniques.[16]

[1]Nonwovens Research Group, Centre for Technical Textiles, School of Design, University of Leeds, Leeds, UK
[2]Institute of Medical & Biological Engineering, University of Leeds, Leeds, UK

Corresponding author:
Elaine R Durham, Nonwovens Research Group, Centre for Technical Textiles, School of Design, University of Leeds, Leeds, LS2 9JT, UK.
Email: E.R.Durham@leeds.ac.uk

Nonwoven scaffolds are assembled from fibres into complex three-dimensional architectures composed largely of through-pores rather than blind or closed pores that are present in other types of porous scaffold (Figure 1). Previous workers have attempted to influence the porosity in electrospun scaffolds,[17–19] however, these approaches can adversely affect mechanical strength.[20] Based on a recently developed water-jet templating technique,[14] it has been found that the internal pore structure and the intrinsic permeability of nonwoven scaffolds can be manipulated by the introduction of multiple tube-like channels within the cross-section. At the same time, surrounding fibres are intensively entangled with each other such that the structure is stable. In simplest form, the channels are periodically spaced tubular voids oriented in parallel. The aim of the present work was to investigate the formation of a new type of nonwoven scaffold wherein a water-jet templating approach[14] was employed to introduce discrete microtubular channels within the porous structure and to study cell penetration in to the interior.

Materials and methods

Scaffold design and production technique

The continuous water jet templating technique[14] involves exposing pre-formed fibre webs to successive rows of constricted high-velocity water jets to simultaneously entwine (bond) and displace fibre segments around an embedded template comprised of closely spaced metal rods or tubes. The cross-sectional shape and dimensions of the template directly influence the geometry of the resulting micro-tubular channels. Following hydroentanglement, the template is physically removed as the fabric slides off the surface leaving continuous channels in the fabric where the templates had once been. In this study, the technique was scaled down and refined to enable the discontinuous production of small scaffold samples (30 mm × 30 mm) containing microtubular channels as small as ~200 μm within the cross-section.

To form the templates, high tenacity polyamide 6 (nylon 6) filament with a diameter of 220 μm was affixed around a thin metal frame and pre-tensioned at a force below the polymer yield point. Adhesive cardboard frames with an internal pre-cut window were then placed on both sides of the metal frame at the filament fixing points. After trimming the filament ends, the metal frame was discarded and the multiple pre-tensioned segments of filament extending across the cardboard frames were secured by adhesive. The frame was then sandwiched between two layers of carded, cross-lapped and pre-needled fabric each of 60 g m^{-2} composed of PLA fibres of 12 μm mean diameter and 38 mm mean fibre length.

To form the scaffold, the combined fibre-template construct was placed on a suctioned water-permeable woven conveyor and exposed to successive hydroentangling injectors (STL Hydrolace system, Leeds) fitted with 120 μm cone capillary nozzles, with a pitch of 90 μm operating at 7 MPa water pressure and a total specific energy of 3 MJ/kg. Residual water was continuously removed by vacuum. Finally, the scaffolds were dried in a convection oven. In addition to the 220 μm templated scaffolds ($n = 10$), control samples ($n = 10$) were produced using identical hydroentangling conditions but with no channels (Figure 2) in addition to a control with no cells and no channels.

The channelled and non-channelled scaffolds were produced with areas of 30 mm × 30 mm and a mean thickness of 2.5 mm. Each scaffold was then cut in half perpendicular to the channels to give a scaffold area of 30 mm × 15 mm. This was carried out prior to the removal of the template to ensure the channel entrances were not disturbed.

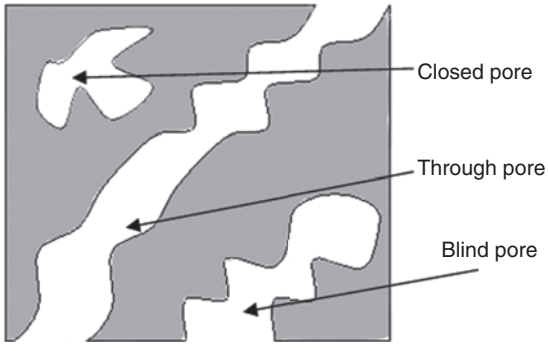

Figure 1. Different pore configurations.

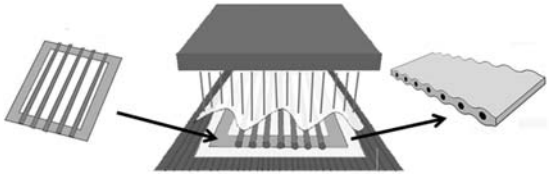

Figure 2. Schematic showing the basic principles of microtubular channel formation in hydroentangled fabrics. A pre-assembled template consisting of closely spaced rigid and incompressible rods (left) is sandwiched between two fibrous webs. The fibres in each layer are simultaneously entangled and deformed around the template rods by incident, high-velocity water jets. Fibres in each web layer become mechanically interconnected by entanglement producing a coherent, porous scaffold structure ($p > 0.9$). Subsequent removal of the template reveals microtubular channels that conform in shape and dimensions to the cross-section of the template rod elements.

Cell culture

Primary human dermal fibroblasts, passage 8 (Cascade), were maintained in monolayer culture, in a humidified atmosphere at 37°C, 5% (v/v) CO_2 in air in Dulbecco's modified Eagle medium (DMEM) supplemented with 10% (v/v) fetal calf serum (FCS), 100 U/mL of penicillin, 100 mg/mL of streptomycin and 2 mM L-glutamine (all Invitrogen). Passaging and preparation of single-cell suspensions for scaffold seeding was achieved by enzymatic digestion using trypsin-EDTA solution (Invitrogen Ltd, UK). Cell counts were assessed using Trypan blue dye (Sigma Aldrich) exclusion and a haemocytometer; live cell numbers were used to determine the final cell density for scaffold seeding.

Scaffold seeding and subsequent culture

To encourage cell attachment to the PLA fibres, scaffolds were soaked in foetal bovine serum (FBS); (Biosera, UK) for 24 h prior to cell seeding. Scaffolds were transferred to sterilised filter paper to remove excess serum (Whatman 40 from Sigma Aldrich) for 15 s prior to cell seeding. The scaffolds were then transferred to individual tissue culture flasks (Nunc branded 25 cm^2 flasks from Thermo Fisher Scientific Ltd). Primary human dermal fibroblasts (HDF, passage 8) suspended in supplemented DMEM were seeded at a density of 1.0×10^6 cells per scaffold into both sides of the scaffolds. To aid cell attachment, the cell suspension was seeded onto the scaffolds 60 min prior to adding supplemented DMEM (6 mL) to ensure that the scaffolds were completely bathed in culture medium. The cell-seeded constructs were cultured at 37°C in 5% CO_2 (v/v) in air. The supplemented medium was changed every 2 days throughout the culture period. Scaffolds were statically cultured *in vitro* for an extended period of up to 14 weeks to assess the long-term stability of the channels and to determine if the channels would remain open and accessible.

Histological analysis

Histological examination was performed on each scaffold (four specimens examined per scaffold), in order to analyse the general histoarchitecture and the cell density and distribution in relation to the channels. The cell-seeded scaffolds were harvested after 11 weeks of culture and fixed in 10% (v/v) neutral buffered formalin (NBF) (Bios Europe Ltd). Post-fixation, samples were dehydrated and embedded in paraffin wax (Bios Europe Ltd). Samples were sectioned to produce sections of 9 μm thickness and transferred to gelatine-coated slides.[21] Histological sections were stained with haematoxylin and eosin (H&E) (Bios Europe Ltd). The stained sections were examined under light microscopy and digital images captured (Olympus BX51, Olympus, UK).

Scanning electron microscope analysis after 14 weeks static cell culture

Statically cultured constructs were harvested for image analysis at week 14 (four specimens per sample). Constructs were removed from culture flasks and gently rinsed using phosphate buffered saline (PBS) (Invitrogen Ltd, UK) to remove any non-adherent cells before being fixed using 2.5% (v/v) gluteraldehyde (Sigma Aldrich) in PBS for 2 h and washed twice, using PBS. Samples were dehydrated using an ascending acetone series: 20%, 40%, 60%, 80%, 100% (v/v), and the samples remained in each grade for 1 h. Constructs were critical point dried using a Polaron E3000 critical point drying apparatus using liquid carbon dioxide as the transition fluid. Each sample was mounted onto a 13-mm diameter pin stub and gold sputter coated (Emscope SC500) before examination. Scanning electron microscope (SEM) samples were imaged at various magnifications between × 25 and × 750. Microscopic analysis was conducted on each of the cultured scaffold types using a Phillips XL30 environmental scanning electron microscope (ESEM) operating in SEM mode.

X-ray microtomography

At week 14, analysis was performed using micro-focused X-ray microtomography (XMT; phoenix X-ray nanotom) to non-destructively examine tissue location and distribution in the scaffold. A well-controlled cone-beam was directed into the sample standing between the X-ray source and a detector. The scan was performed at a resolution of 2 μm per voxel. During the scan, the sample was rotated for 360° at an angle rate of 0.25°/step, and 1440 projection images were recorded. The voltage, current and irradiation time used were optimised for the best contrast among the sample components, with values of 80 kV, 100 μA and 1000 milliseconds, respectively. The projection images obtained were computationally reconstructed (phoenix X-ray nanotom) to produce a three-dimensional spatial image.

Results

Scaffold manufacture

Scaffolds containing internal channels were successfully produced by the new production technique. A cross-section of a scaffold produced by the new method, with the filament templates still in place, is shown in

Figure 3. The successful interconnection of the two fibrous PLA fibre layers and the shaping of the channels around the filament templates was confirmed by SEM analysis (Figure 4(a)). In this image, the template spacing was of the order of 1000 μm. Following their removal from the scaffold, the channels remained open at their extremities (Figure 4(b)), providing a highly accessible, low tortuosity pathway for cell penetration during seeding and for the diffusion of culture medium. Although some fibres were migrated around the perimeter of the channel, clearly demarcating its boundary, this was not the case for all fibres (Figure 4(c) and (d)).

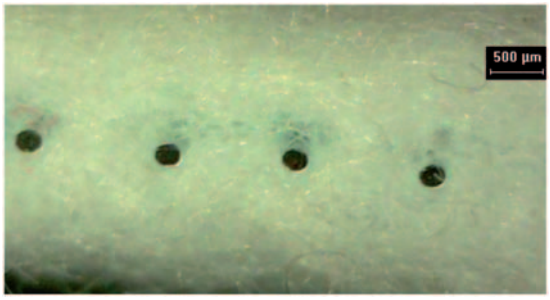

Figure 3. Cross section of a microtubular channelled fabric immediately prior to removal of the template; filament diameter = 200 μm. Fibres are entangled around and between the filaments.

Histological analysis

Histological examination was performed on scaffold quarters, in order to analyse the general histoarchitecture, and the cellular distribution in relation to the channels. The analysis showed that there was a greater density of cells in the centre of the channelled scaffolds than in the centre of the non-channelled scaffolds after 11 weeks. No biological changes were observed in the no cell control at week 11. It is likely that the greater density of cells in the centre of the channelled scaffold compared to the nonchannelled scaffold was due to an increased supply of nutrients and oxygen. However, additional studies of cell behaviour in the scaffolds (over a shorter time period and not reported here) suggested that the channels may also aid the initial migration of cells into the centre of the scaffold. As the cells had not migrated away from the centre of

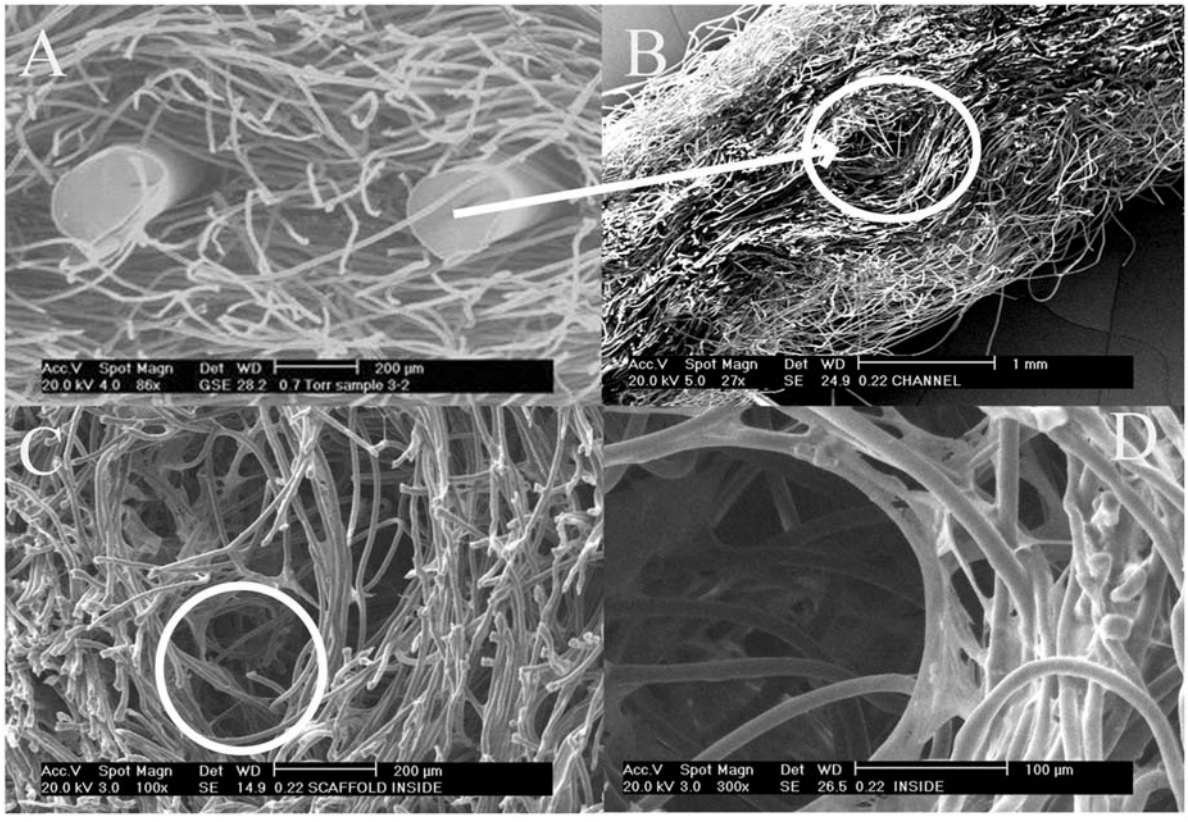

Figure 4. Microstructure of the channelled scaffold. (A) Scaffold cross-section showing two rods in situ. (B) Channel entrance after removal of template. (C) Interior of the scaffold (channel position circled). (D) Curved fibre segments around the periphery of a channel.

the scaffold (in the 14-week period), it could be suggested that the greater density of cells in the centre of the channelled scaffold was as a result of the combination of both factors.

Stability of channels after 14 weeks static cell culture

Even after an extended period of cell culture (14 weeks), the channel entrances remained open and were not occluded with ECM. The channels were easily identifiable in sections of the scaffold and were characterised by the presence of curved fibre segments around their periphery (Figure 5). Both the channelled and nonchannelled scaffolds appeared to have good long-term stability although compression testing was outside the remit of this study. The fibres, which would have been in the channel areas, had simply been displaced to the area immediately surrounding the channels (thereby reinforcing the channel wall area). By contrast, the pores in the surrounding scaffold surface were

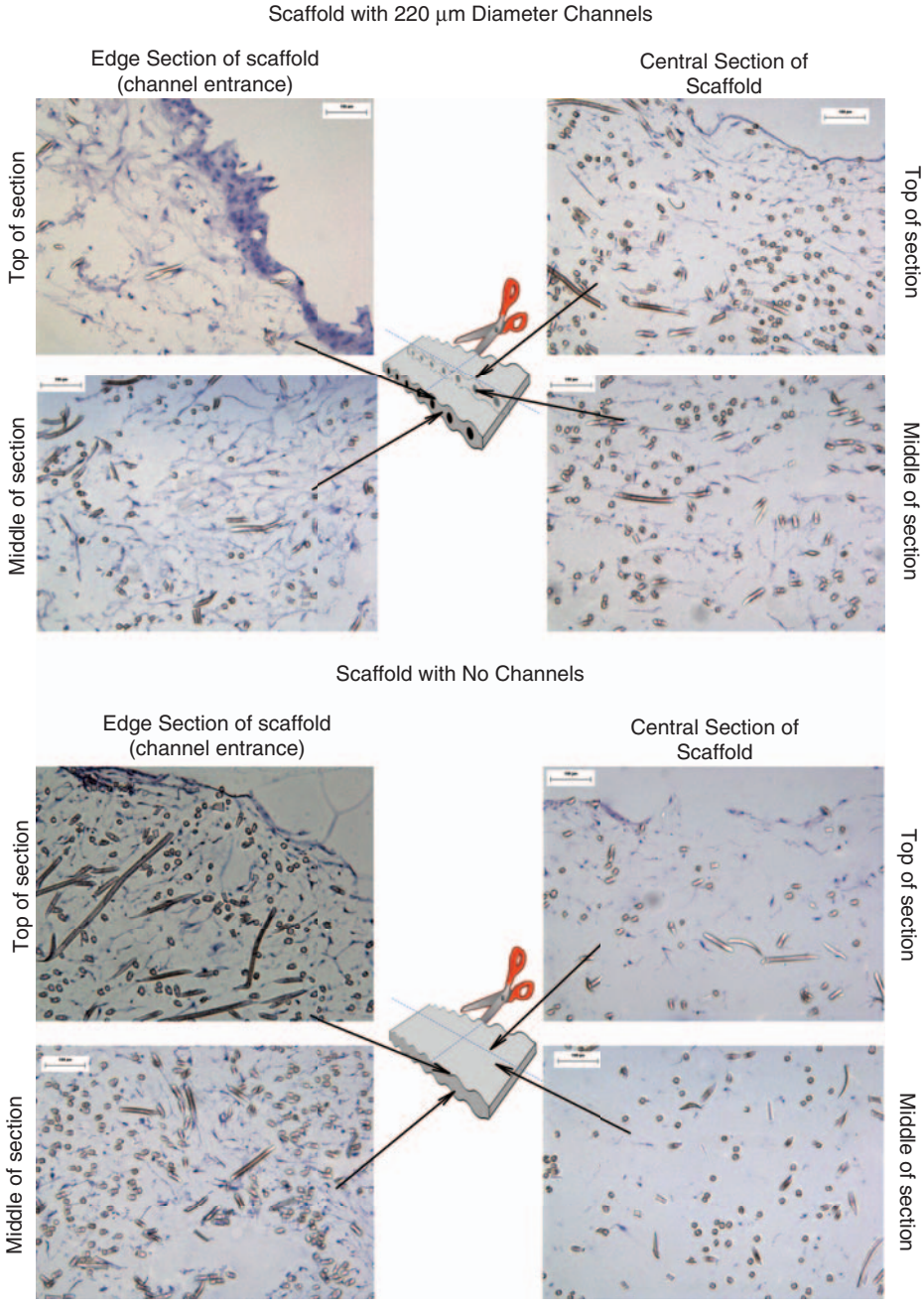

Figure 5. Sections of channelled and non-channelled scaffolds stained with hematoxylin and eosin (H&E) at week 11 (static culture). A higher density of cells at the centre of the channelled scaffold is visible (compare Image D with Image H), all images × 100 mag.

extensively in-filled with ECM (Figure 5). The interior of a channel in the core of the scaffold, showing clear evidence of cell/matrix deposition within its walls after 14 weeks, is shown in Figure 5(d). No biological changes were observed on the no cell control scaffolds. The PLA fibres used in this study were of a textile grade, and as part of another study (not reported here), the scaffolds were shown not to degrade in a 14-week time period under comparable culture conditions.

XMT imaging of the scaffolds after 14 weeks static cell culture

The XMT studies permitted the scaffold to be probed in three dimensions to locate the channels and in two dimensions to assess cell and matrix deposition without disturbing the structure. Identification of the fibre and ECM components relied on differences in the linear attenuation coefficients, which is based on the relative density of the materials. In Figure 6, the ECM sheet structure is shown as red and the fibres in white. Whilst matrix was concentrated in the scaffold exterior (Figure 6(c)), small areas of matrix were also present in the scaffold interior in all of the 2D sections (Figure 6(a)and (b)) and between channels in the cross-section (Figure 6(d)). Using XMT, we were not able to be more specific about the components of the matrix, however, antibody labelling (not reported here) was shown to be positive for the specific matrix markers of collagen I, collagen IV and fibronectin.

Discussion

One of the limitations of conventional nonwoven scaffold fabrication has been the problem of precisely controlling pore size and constructing well-defined internal channels with the scaffold.[22] Previously, channelling of porous scaffolds to improve cell penetration, nutrient and gas exchange has been mainly confined to nonfibrous scaffold assemblies using techniques such as sponge, foam and hydrogel scaffolds.[9–11] Although well-defined channels or grooves have been introduced into a range of assemblies, at a scale appropriate for tissue engineering,[23] the tortuous nature of the pores[24] (or lack of pores) in the area surrounding the channel

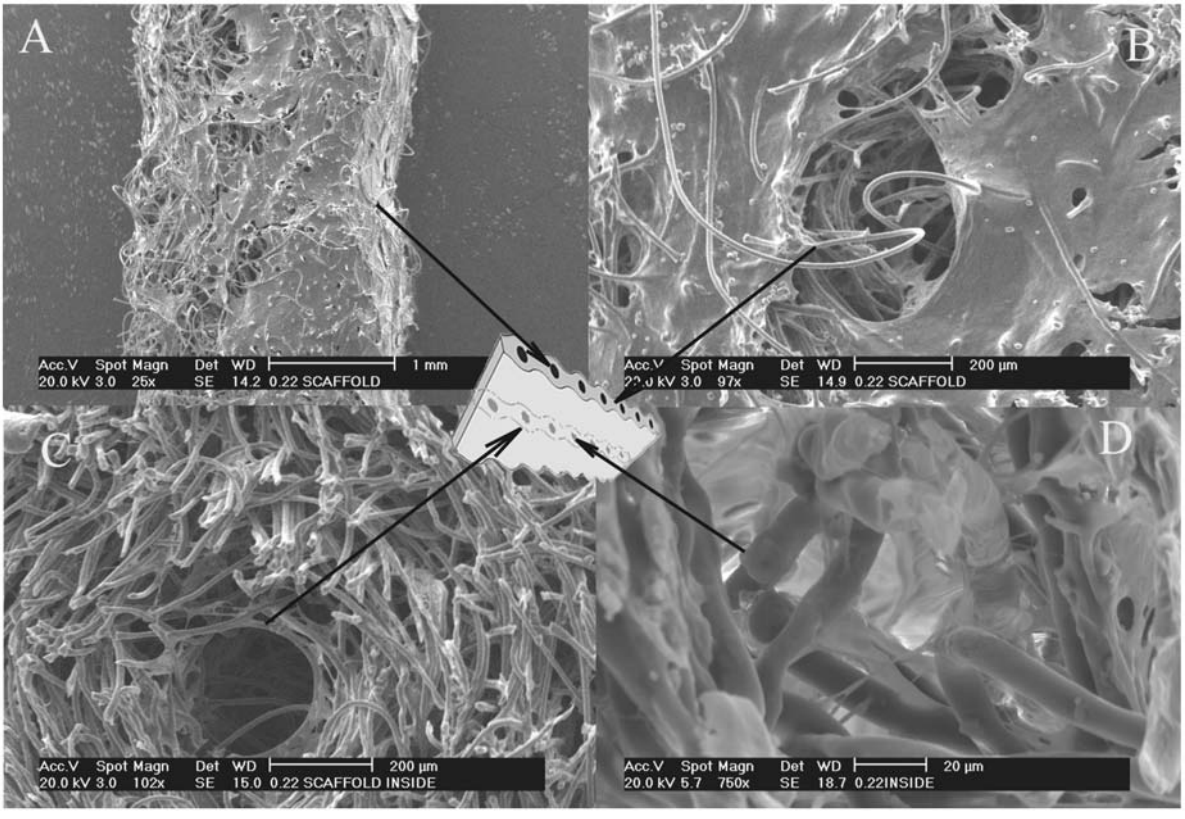

Figure 6. Scanning electron microscope (SEM) images of 200 µm channelled scaffolds after 14 weeks of cell culture. (A) Macro-view showing channel entrances running vertically through the centre of the image × 25 mag; (B) Channel entrance × 97 mag; (C) Internal view, × 25 mag; (D) Internal view of the scaffold showing cell/matrix deposition around the interior walls of the channel, × 750 mag.

can limit their functional performance as a scaffold. Nonwoven materials are largely composed of interconnecting pores,[25] which would be expected to enhance the communication between the channel walls and the surrounding porous structure. Some of the existing approaches for introducing channels involves the utilisation of a sacrificial component that is removed by chemical dissolution[15] or thermal degradation[26] after the bulk scaffold structure has been stabilised. A challenge with such methods is to eliminate potentially cytotoxic residues without modifying the structure of the as-formed scaffold.

The technique described herein utilised a solid template and involved scaling-down an industrial hydroentangling process to facilitate the continuous or semi-continuous manufacture of fibrous scaffolds comprised of resorbable fibres, in this example: PLA. The feasibility of creating well-defined microtubular channels within a nonwoven scaffold cross-section using this approach has been successfully demonstrated. The incident water jets consolidate the fibrous structure and migrate fibre segments within the web structure around the fixed templates (Figure 3) whilst entwining and knotting of proximal fibres to produce a coherent structure (Figure 4) Fibre entanglement is influenced by vortices in the fluid bed surrounding the fibres, which gives rise to fibre bending, rotation and displacement. The flexural and torsional rigidities of fibres will therefore influence the degree of entanglement and fabric strength that can be generated for a specific energy input. In terms of engineering fibre properties to ensure compatibility with this process, the diameter, density, tensile modulus and shape factor of the fibres will directly influence their flexibility.[27]

The viability of cells is dependent on their proximity to the nutrient and oxygen supply and the maximum communication distance is a function of cell type. For example, chrondocytes have a relatively low oxygen requirement and as a result, cartilage is one of the few soft tissues to have been grown *in vitro* to thick cross-sections of more than 1 mm without the use of channels, microfluidics or complex scaffold constructs.[28] Dermal fibroblasts grown in dense, three-dimensional collagen scaffolds containing fluidic channels showed significantly elevated cell viability compared to scaffolds without any channels.[29] In the present work with primary human dermal fibroblasts, the conditions for cell penetration and cell viability were particularly challenging because of the thickness of the scaffolds (2.5 mm) and the length of the culture period (up to 14 weeks), which resulted in extensive occlusion of the exterior pore openings by ECM. Although cells were concentrated on the scaffold's exterior surface's at weeks 11 and 14, there was a greater through-thickness distribution of cells within the channelled scaffold suggesting that conditions for nutrient and gas exchange had been improved. A higher density of cells was observed in the interior of channelled scaffold than the scaffold with no channels at week 11 (Figure 7(d) and (h)). Cells were also located within the interior walls of the channels after week 14 supporting the hypothesis that when filled with medium the channels provided effective pathways for molecular diffusion (Figure 5(d)). Natural tissue is not a homogeneous structure as it has areas of dense matrix and areas of less-dense matrix. This would suggest that it is not necessary to have a homogenous scaffold. In addition to the channelled areas, there were still large parts of the scaffold where the cells were fully supported by the fibrous pore structure and could lay down matrix.

The relatively large diameter of the channel entrances ($\sim$220 μm) prevented the cellular bridging and infiltration that was evident over large areas of the surrounding scaffold structure. Thus, it may be expected that if the channel diameter were reduced to a critical value that approximated to the pore dimensions of the fibrous nonwoven scaffold, the channel entrances would rapidly become occluded and therefore unavailable as a means to improve transport to the scaffold interior.

In addition to channel entrance dimensions, channel shape is thought to be important. A numerical analysis by Ahn et al.[30] showed that a channel with a uniform diameter, (cylinder shaped) and a channel with a diameter gradient, (cone shaped) produced different oxygen concentrations. In their study, cell culture experiments revealed that cell proliferation and viability were superior in the constructs and scaffolds containing cone-shaped channels.

A further consideration is the proximity of channels and its effect on cell penetration and viability.[31] Few cells tolerate distances of greater than 200 μm from a blood vessel[32] and in the present scaffolds, the interval spacing between the channels was $\sim$1000 μm, which is above this critical maximum distance. Despite this, because the channel entrances remained open and unoccluded (Figure 5), access to nutrient and oxygen may have still been available during *in vitro* cell culture despite extensive occlusion by ECM of the pore openings in the scaffold exterior. In the present scaffold production technique, the channel spacings may be readily adjusted by varying the placement of the filaments in the template and this will be necessary to improve scaffold functionality. In preliminary studies (unpublished), the smallest spacing between adjacent channels that could be obtained whilst still maintaining a strong interconnection between the fibres of the upper and lower webs was $\sim$250 μm. Further reductions in the channel spacing may be possible by reducing the nozzle dimensions and pitch of the water jets as well

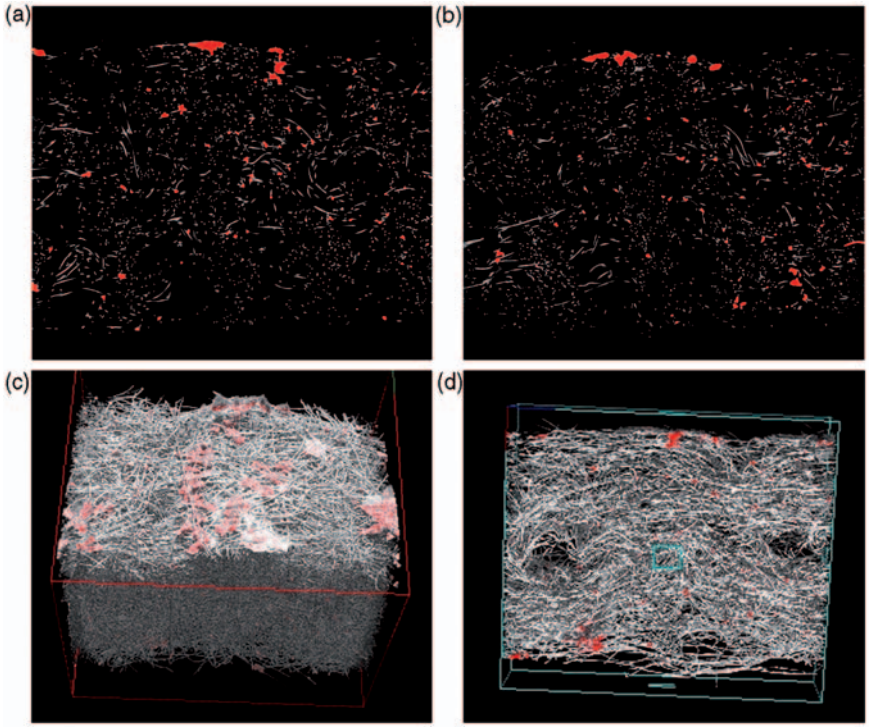

Figure 7. X-ray microtomography (XMT) images of 200 μm channelled scaffolds after 14 weeks of cell culture. (A) and (B) 2D views in the interior of the scaffold; (C) 3D view; (D) Cross section showing the channels. The fibres are white and the red sheet structures are biological matrix.

as by reducing the mean fibre diameter in the original webs.

Conclusions

A new template-hydroentangling technique has been presented for the assembly of nonwoven scaffolds containing channels that have a fully interconnected pore structure. The process does not involve cytotoxic solvents or adhesives. In this case study, three-dimensional scaffolds comprised of PLA were produced containing well-defined micro-tubular channels within the scaffold cross-section. The channels were found to promote the penetration and distribution of primary human dermal fibroblasts inside the scaffold. The channel entrances remained open and unoccluded by ECM after culture *in vitro* after 14 weeks.

Funding

The authors are supported by the Leeds Centre of Excellence in Medical Engineering funded by the Wellcome Trust and EPSRC, WT088908/z/09/z.

Acknowledgements

Professor S. J. Russell is a director and shareholder of NIRI Ltd., to which the Hydrospace technology is assigned.

A version of this paper has been previously presented at the Edana Nonwovens Research Academy, Aachen, Germany, 2010.

References

1. Mikos AG, Lu L, Temenoff JS, et al. Synthetic bioresorbable polymer scaffold. In: Ratner BD, Hoffman AS, Schoen FJ and Lemons JE (eds) *Biomaterials science—an introduction to materials in medicine*, 2nd ed. San Diego, CA: Elsevier Academic Press, 2004, p.735.
2. Yang S, Leong KF, Du Z, et al. The design of scaffolds for use in tissue engineering. Part 1. Traditional factors. *Tissue Eng* 2001; 7: 679–689.
3. Edwards SL. *Design of nonwoven scaffold for the tissue engineering of the anterior cruciate ligament*. PhD Thesis, University of Leeds, UK, 2005.
4. Freed LE, Martin I and Vunjak-Novakovic G. Frontiers in tissue engineering; *in vitro* modulation of chrondrogenesis. *Clin Orthop Rel Res* 1999; 367S: S46–S58.
5. Kannan RY, Salacinski HJ, Sales K, et al. The roles of tissue engineering and vascularisation in the development of micro-vascular networks: a review. *Biomaterials* 2005; 26: 1857–1875.
6. Kaihara S, Borenstein J, Koka R, et al. Silicon micromachining to tissue engineer branched vascular channels for liver fabrication. *Tissue Eng* 2000; 6: 105–117.

7. Sachlos E, Gotora D and Czernuszka JT. Collagen scaffolds reinforced with biomimetic composite nano-sized carbonate-substituted hydroxyapatite crystals and shaped by rapid prototyping to contain internal microchannels. *Tissue Eng* 2006; 12: 2479–2487.
8. Sachlos E, Reis N, Ainsley C, et al. Novel collagen scaffolds with predefined internal morphology made by solid freeform fabrication. *Biomaterials* 2000; 21: 2443–2452.
9. Rose FR, Cyster LA, Grant DM, et al. *In vitro* assessment of cell penetration into porous hydroyapatite scaffolds with a central aligned channel. *Biomaterials* 2004; 25: 5507–5514.
10. Silva MMCG, Cyster LA, Barry JJA, et al. The effect of anisotropic architecture on cell and tissue infiltration into tissue engineering scaffolds. *Biomaterials* 2006; 27: 5909–5917.
11. Radisic M, Park H, Chen F, et al. Biomimetic approach to cardiac tissue engineering: oxygen carriers and channelled scaffolds. *Tissue Eng* 2006; 12: 2077–2091.
12. Gao J, Crapo PM and Wang Y. Macroporous elastomeric scaffolds with extensive micropores for soft tissue engineering. *Tissue Eng* 2006; 12: 917–925.
13. Murphy WL, Dennis RG, Kileny JL, et al. Salt fusion: an approach to improve pore interconnectivity within tissue engineering scaffolds. *Tissue Eng* 2002; 8: 43–52.
14. Russell SJ, Pourmohammadi A, Mao N, et al. *Nonwoven spacer fabric*. Patent 2007/0059496 A1, USA, 2007.
15. Nazhat SN, Abou Neel EA, Kidane A, et al. Controlled microchannelling in dense collagen scaffolds by soluble phosphate glass fibers. *Biomacromolecules* 2007; 8: 543–551.
16. Ma PX and Zhang R. Microtubular architecture of biodegradable polymer scaffold. *J Biomed Mater Res* 2001; 56: 467–477.
17. Ju YM, Choi JS, Atala A, et al. Bilayered scaffold for engineering cellularized blood vessels. *Biomaterials* 2010; 31: 4313–4321.
18. Wang JP, Valmikinathan CM, Liu W, et al. Spiral-structured, nanofibrous, 3D scaffolds for bone tissue engineering. *J Biomed Mater Res* 2010; 93A: 753–762.
19. Nam J, Huang Y, Agarwal S, et al. Improved cellular infiltration in electrospun fiber via engineered porosity. *Tissue Eng* 2007; 13: 2249–2257.
20. Baker BM, Nerurkar NL, Burdick JA, et al. The potential to improve cell infiltration in composite fiber-aligned electrospun scaffolds by the selective removal of sacrificial fibers. *Biomaterials* 2008; 29: 2348–2358.
21. Bancroft JD and Gamble M. *Theory and practice of histological techniques*, 6th edn. Edinburgh: Churchill Livingstone, 2007.
22. Sachlos E and Czernuszka JT. Making tissue engineering scaffolds work. Review on the application of solid freeform fabrication technology to the production of tissue engineering scaffolds. *Eur Cell Mater* 2003; 5: 29–40.
23. Vernon RB, Gooden MD, Lara SL, et al. Microgrooved fibrillar collagen membranes as scaffolds for cell support and alignment. *Biomaterials* 2005; 26: 3131–3140.
24. Yoon B-H, Koh Y-H, Park C-S, et al. Generation of large pore channels for bone tissue engineering using camphene-based freeze casting. *J Am Ceram Soc* 2007; 90: 1744–1752.
25. Edwards SL, Church JS, Alexander DLJ, et al. Modeling tissue growth within nonwoven scaffolds pores. *Tissue Eng C* 2011; 17: 123–130.
26. Golden AP and Tien J. Fabrication of microfluidic hydrogels using molded gelatin as a sacrificial element. *Lab Chip* 2007; 7: 720–725.
27. Morton WE and Hearle JWS. *Physical properties of textile fibres*, 2nd edn. Manchester: The Textile Institute, 1975.
28. Freed LE, Hollander AP, Martin I, et al. Chondrogenesis in a cell-polymer-bioreactor system. *Exp Cell Res* 1998; 240: 58–65.
29. Lee W, Lee V, Polio S, et al. On-demand three-dimensional freeform fabrication of multi-layered hydrogel scaffold with fluidic channels. *Biotechnol Bioeng* 2010; 105: 1178–1186.
30. Ahn G, Park JH, Kang T, et al. Effect of pore architecture on oxygen diffusion in 3D scaffolds for tissue engineering. *J Biomech Eng* 2010; 132: 104506.
31. Karande TS, Ong JL and Agrawal CM. Diffusion in musculoskeletal tissue engineering scaffolds: design issues related to porosity, permeability, architecture, and nutrient mixing. *Ann Biomed Eng* 2004; 32: 1728–1743.
32. Muschler GE, Nakamoto C and Griffith LG. Engineering principles of clinical cell-based tissue engineering. *J Bone Joint Surg Am* 2004; 86A: 1541–1558.